Asian Journal of Chemistry; Vol. 24, No. 9 (2012), 4068-4070

ASIAN JOURNAL OF CHEMISTRY

www.asianjournalofchemistry.co.in

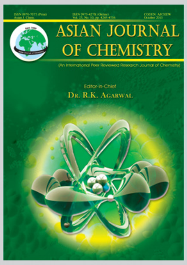

Synthesis and Electrochemical Properties of $BaCe_{0.8}Gd_{0.2}O_3$ Protonic Conductor†

JIHAI CHENG* and CHANGAN TIAN

Department of Chemistry and Materials Engineering, Hefei University, Hefei 230022, P.R. China

*Corresponding author: E-mail: cjh@hfuu.edu.cn

AJC-11318

Gadolinium-doped barium cerate ($BaCe_{0.8}Gd_{0.2}O_3$, BCG) powders were prepared by the sol-gel auto-combustion process. According to the X-ray diffraction analysis, the formed $BaCe_{0.8}Gd_{0.2}O_3$ powders with perovskite structure are orthorhombic phase. When doped with larger sized Gd^{3+} ions and higher dopant concentration, the orthorhombic barium cerate lattice expanded. Results revealed that $BaCe_{0.8}Gd_{0.2}O_3$ proton-conducting solid electrolyte showed higher sinterability, its conductivity increased with the increase of the sintering temperature and a total conductivity 7.49×10^{-3} S/cm at 800 ºC could be obtained.

Key Words: Fuel cells, Protonic conductor, Electrical conductivity, Perovskite.

INTRODUCTION

Solid oxide fuel cell (SOFC) has increasingly attracted interest as an effective mean for generating electricity due to its high-energy efficiencies, silent work and low impact to environment[1,2]. Research and development electrolyte materials for solid oxide fuel cell operating at intermediate temperature have received much attention.

Perovskite oxides based on doped ABO_3 have been studied as electrolytes in solid oxide fuel cell owing to their high proton conductivity at low temperatures[3,4]. The doped $BaCeO_3$ oxides display high proton conductivity values in humid hydrogen at elevated temperatures[5-7] and these perovskite-structure compounds have been considering as one of the best candidates to replace the yttria-stabilized zirconia (YSZ) electrolyte for solid oxide fuel cell[8,9].

EXPERIMENTAL

Analytical pure $Ce(NO_3)_3$, $Ba(NO_3)_2$ and Gd_2O_3 were used as starting materials. $Ce(NO_3)_3$ and $Ba(NO_3)_2$ were dissolved into deionized water, Gd_2O_3 was dissolved into solution of nitric acid. The two liquid were mixed together. Citric acid was then added as chelating agent, the citric acid/metal molar ratio was fixed at 1.5. The pH value of the mixture was adjusted to 6 by $NH_3{\cdot}H_2O$ in order to achieve full complexing citric acid with metallic ions without precipitation. This mixed solution was then heated under stirring at 60 ºC and homogeneous sol was formed, converted to a viscous gel. Wet gel was further heated to 120 ºC to remove the solvents and the dried gel was baked in an oven at 500-700 ºC, where the auto-combustion reaction took place to form the precursors. The powders were prepared by calcining the precursors at 800-1000 ºC for 3 h. The resulting powders were pressed into pellets and sintered at different temperatures in air atmosphere for 4 h, respectively.

The crystal structure of the calcined powders was determined by X-ray diffraction. Relative density of the sintered pellets was measured using the Archimedes method. The measurement of AC impedance was performed in air with an electrochemical workstation CHI660B. The frequency range varied from 0.1 Hz to 100 kHz, the measurement curves were conducted in the temperature range from 500-800 ºC with an interval of 50 ºC.

RESULTS AND DISCUSSION

Phase formation: Fig. 1 shows the X-ray diffraction patterns of $BaCe_{0.8}Gd_{0.2}O_3$ powders. The results show that $BaCO_3$, CeO_2 and Gd_2O_3 are the major crystalline phase between 800 and 900 ºC (Fig. 1a-b). On the other hand, the $BaCeO_3$ phase starts to occur above 900 ºC and until temperature reaches 1000 ºC, the phase becomes pure $BaCeO_3$ (Fig. 1c). All diffraction peaks match well with JCPDS file No. 82-2425, indicating the substitution of Gd^{3+} ions to Ce^{4+} sites has taken place, the Gd^{3+} ions dissolved in the crystal lattice of $BaCeO_3$ completely and formed $BaCe_{0.8}Gd_{0.2}O_3$ powders with single orthorhombic perovskite phase.

---

†Presented to The 5th Korea-China International Conference on Multi-Functional Materials and Application.

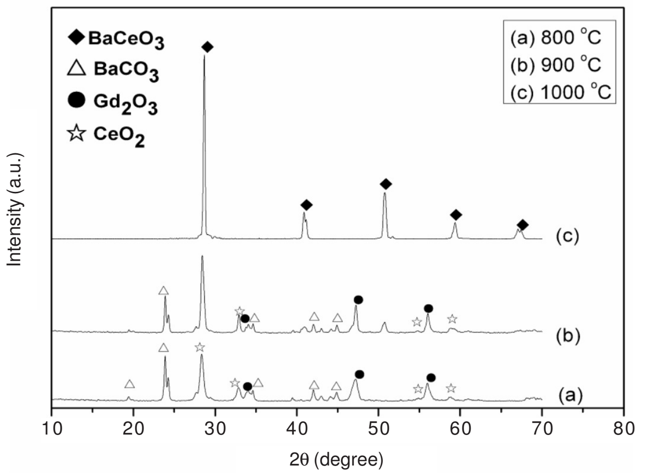

Fig. 1. X-Ray diffraction patterns of $BaCe_{0.8}Gd_{0.2}O_3$ powders sintered at: (a) 800 °C, (b) 900 °C and (c) 1000 °C

Sintering behaviours: Fig. 2 shows the relative density of $BaCe_{0.8}Gd_{0.2}O_3$ ceramics sintered at different temperatures and soak times. The density of sintered $BaCe_{0.8}Gd_{0.2}O_3$ ceramics increased with sintering temperature and a density of 6.096 g/cm^3 measured by Archimedes method was found in the 1350 °C samples, which indicated that the practical density is 95.5 % sintered referenced to the theoretical density (6.383 g/cm^3)[10]. Furthermore, when sintering temperature is above 1350 °C, the relative density of sintered $BaCe_{0.8}Gd_{0.2}O_3$ ceramic can hardly improve.

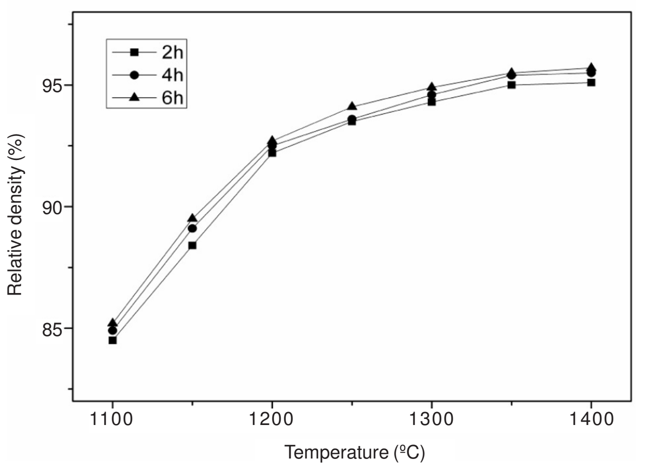

Fig. 2. Dependence of relative density on sintering temperatures for $BaCe_{0.8}Gd_{0.2}O_3$ ceramics

Electrical conductivity: The total resistance and conductivity data of electrolyte obtained from the AC impedance spectra are compiled in Table-1.

The conductivity data were analyzed further using the conventional Arrhenius equation. Fig. 3 shows the Arrhenius plots of the electrolyte conductivity for the sample in the temperature range 500-800 ºC. Although there are significant uncertainties in the electrolyte resistance estimated from the impedance data. The Arrhenius plots are on a logarithmic scale and activation energies can still be estimated reasonably well.

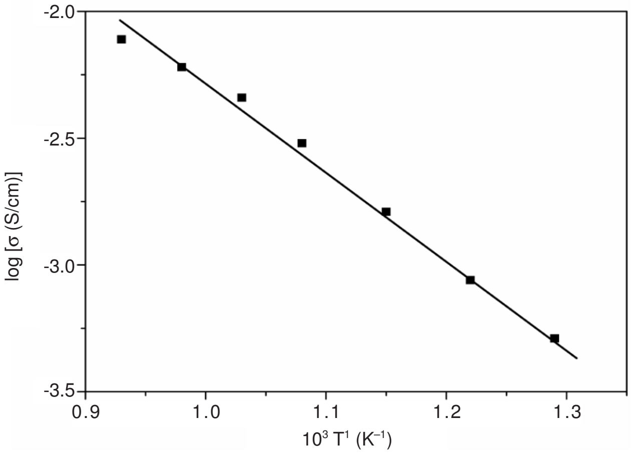

Fig. 3. Arrhenius plot comparing the total electric conductivity of $BaCe_{0.8}Gd_{0.2}O_3$

The high-frequency of the electrochemical workstation is insufficient and resulted in an incomplete semicircle, which makes it difficult to determine the grain resistance and the grain-boundary resistance. Although significant uncertainties exist in the electrolyte resistance estimated from the impedance data, the activation energies for $BaCe_{0.8}Gd_{0.2}O_3$ samples can be obtained from Arrhenius plots (Fig. 3). The activation energy of the $BaCe_{0.8}Gd_{0.2}O_3$ sample was estimated to be 0.95 eV.

The total conductivity of $BaCe_{0.8}Gd_{0.2}O_3$ ceramics measured in 500-800 ºC range are shown in Fig. 4. There is a significant difference in the conductivities between the lower temperature (1200-1300 ºC) and higher temperature (1350-1400 ºC) sintered samples. Higher conductivity is found in higher temperature sintered $BaCe_{0.8}Gd_{0.2}O_3$ ceramics because of the larger density and grain size[5,11]. A total conductivity 7.49 × 10^{-3} S/cm at 800 ºC could be obtained in 1350 ºC sintered $BaCe_{0.8}Gd_{0.2}O_3$ sample. However, when the sintering temperature exceeded 1350 ºC, the conductivity can hardly increase. The reason is attributed to the lattice oxygen loss of this system at high temperatures caused the stagnation or decrease of electrical conductivity due to the reduction of charge carrier concentration[12].

Conclusion

The sol-gel auto-combustion process was used to synthesize perovskite-type $BaCe_{0.8}Gd_{0.2}O_3$ ceramic proton-conducting solid electrolyte. The phase formation, sintering behaviours and electrochemical properties were investigated. The result indicated that, when doped with larger sized Gd^{3+} ions, the perovskite lattice of $BaCeO_3$ expanded. $BaCe_{0.8}Gd_{0.2}O_3$ samples show superior sinterability. The total conductivity of 7.49 ×

TABLE-1
RESISTANCE AND ELECTRICAL CONDUCTIVITY OF $BaCe_{0.8}Gd_{0.2}O_3$ AT VARIOUS TEMPERATURES

T (ºC)	500	550	600	650	700	750	800
R (Ω)	525.4	129.3	35.13	18.63	12.52	9.30	7.56
σ (S/cm)	1.08 × 10^{-4}	4.38 × 10^{-4}	1.61 × 10^{-3}	3.04 × 10^{-3}	4.52 × 10^{-3}	6.08 × 10^{-3}	7.49 × 10^{-3}

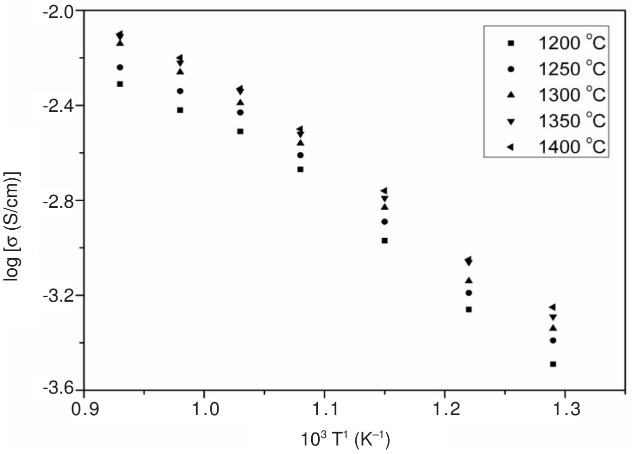

Fig. 4. Dependence of the conductivity on temperature for $BaCe_{0.8}Gd_{0.2}O_3$ ceramics

10^{-3} S/cm at 800 ºC could be obtained in $BaCe_{0.8}Gd_{0.2}O_3$ protonic conductor.

ACKNOWLEDGEMENTS

This work was kindly supported by the Nature Science Foundation of Anhui Province contract No. 10040606Q53 and the National Natural Science Foundation of China under grant No. 51102073.

REFERENCES

1. E. Caproni, D. Gouvea and R. Muccillo, *Ceram. Int.*, **37**, 273 (2011).
2. L. Bi, S.Q. Zhang, S.M. Fang, L. Zhang, K. Xie, C.R. Xia and W. Liu, *Electrochem. Commun.*, **10**, 1005 (2008).
3. J.-H. Kim, B. Tsuchiya, S. Nagata and T. Shikama, *Solid State Ionics*, **180**, 271 (2009).
4. T. Ohzeki, S. Hasegawa, M. Shimizu and T. Hashimoto, *Solid State Ionics*, **180**, 1034 (2009).
5. Y.C. Liou and S.L. Yang, *J. Power Sources*, **179**, 553 (2008).
6. T. Oh, J.L. Li, H.S. Yoon and E.D. Wachsman, *Ionics*, **15**, 525 (2009).
7. L. Bi, S. Fang, Z. Tao, S.Q. Zhang, R.R. Peng and W. Liu, *J. Eur. Ceram. Soc.*, **29**, 2567 (2009).
8. E. Gorbova, V. Maragou, D. Medvedev, A. Demin and P. Tsiakaras, *J. Power Sources*, **181**, 207 (2008).
9. A.K. Azad and J.T.S. Irvine, *Solid State Ionics*, **178**, 635 (2007).
10. Z.J. Li, R.Q. Liu, J.D. Wang, Y.H. Xie and F. Yue, *J. Solid State Electrochem.*, **9**, 201 (2005).
11. A. Bassano, V. Buscaglia, M. Viviani, M. Bassoli, M.T. Buscaglia, M. Sennour, A. Thorel and P. Nanni, *Solid State Ionics*, **180**, 168 (2009).
12. H. Zhao, D. Teng, X. Zhang, C. Zhang and X. Li, *J. Power Sources*, **186**, 305 (2009).